Study of Efficiency of Ka-band IMPATT Diodes and Oscillators around Optimized condition

Tapas Kumar Pal[1] and J. P. Banerjee[2]

[1]*Research Centre Imarat, Vignyana Kancha*
Hyderabad – 500 069, INDIA.
E-mail: tkp_007@rcilab.in

[2]*Institute of Radiophysics and Electronics*
University of Calcutta, Kolkata – 700009,
E-mail:jpbanerjee06@rediffmail.com

Abstract

The device efficiency of a silicon SDR (p^+nn^+) IMPATT diode at Ka-band has been studied by using small signal simulation and field swing upto 50 % of the maximum dc electric field. It is found that the d.c. to r.f. conversion efficiency of the SDR IMPATT diode decreases with the increase in field swing upto 50 %, from 8.98% to 7.84%. An integrated heat sink cum resonant cap cavity has been used for Ka-band oscillator in the present simulation. RF measurements have been performed on a silicon Ka-band SDR (p^+nn^+) IMPATT diode embedded in the cavity. Simultaneous electronic and mechanical tuning of the oscillator has been carried out to optimize the frequency and generated r.f. power output over the operating range of input d.c. bias current. An optimized r.f. power output of 180 mW has been obtained from the oscillator with an input d.c. bias current 190 mA. The measured output power has been co-related with theoretical estimated r.f. power obtained from simulation from which the efficiency of the resonant cap oscillator has been obtained.

Key words: *Circuit efficiency, Device efficiency, Electronic tuning, IMPATT diode, Mechanical tuning, Small signal simulation.*

1. Introduction

IMPact **A**valanche **T**ransit **T**ime (IMPATT) device has already emerged as the most powerful solid-state device for generation of high CW and pulsed power at millimeter wave frequencies [1], [2]. The device also provides high oscillator output power with high DC to RF conversion efficiency for Silicon Monolithic Millimeter Wave Integrated Circuits (SIMMWIC) [3]. First, the authors have done the DC and small signal simulation of silicon SDR (p^+nn^+) IMPATT diodes at Ka-band, starting from the field maximum point in the depletion layer. The device efficiency has been calculated using Scharfetter and Gummel expression [4] which holds good up to 50% field swing of the maximum d.c. electric field. The authors used an integrated heat sink cum resonant cap cavity for Ka-band oscillator [5-6]. Since resonant cap structure has been used in microwave and millimeter wave systems for

mounting active semiconductor device mainly because of its simplicity of mechanical construction, easy tunability and lower cost compared to other mounting circuits. A large number of studies have been made on this circuit structure over long period of time. Large mechanical tuning band was found [7] by varying the sliding back short tuner for a millimeter wave cap-type IMPATT oscillator. Almost similar type of work was done on mechanical tuning [8]. But these studies did not include the electronic tuning behavior of the IMPATT oscillator. Later Swartz et al [9] conducted a thorough and detailed study on a p-type SDR silicon IMPATT diode housed in a resonant cap circuit over the Ka-band (26.5-40 GHz). In that study, they found maximum oscillator power output of nearly 700 mW with a power conversion efficiency of 10.9%. But their work does not provide an insight into the power generated by the diode chip itself.

In the present study, CW measurements on a Ka-band IMPATT oscillator using a resonant cap structure and silicon SDR (p^+nn^+) IMPATT have been carried out to find the optimum r.f. power output and corresponding frequency of the oscillator. Electronic and mechanical tuning with simultaneous variation of the d.c. input current and back short tuner position of the oscillator have been carried out to optimize the oscillation frequency and r.f. power output. It has been found that an optimized r.f. power output of maximum 180 mW could be obtained from the oscillator at an input d.c. bias current of 190 mA. A computer simulation for operation of a standard Ka-band silicon SDR (p^+nn^+) type IMPATT diode has been made to find an estimated r.f. power generated by the IMPATT diode. The estimated power from IMPATT diode has been found in the range of 444 mW to 391 mW when the signal amplitude was varied from small signal case to a maximum of 50% of maximum d.c. electric field. A calculation of circuit efficiency w.r.t. optimum oscillator output power for various field swings has been made. Thus a range of circuit efficiency between 41.18% to 46.03% has been achieved.

2. DC and Small Signal Simulation

The authors have considered one-dimensional model of a reverse biased *p-n* junction for DC and Small signal simulation [10] of silicon SDR ($p^+ nn^+$) IMPATT diode, schematically shown in Figure 1, having symbols with usual meanings. The total current is composed of conduction current and displacement current only because the diffusion current is negligibly small. The total current density is given by the expression:

$$J_{total} = q.\left(n.v_{sn} + p.v_{sp}\right) + \frac{\delta(\varepsilon E)}{\delta t} \quad (1)$$

The spatial variation of electric field in the space charge layer is obtained from Poisson's equation as

$$\frac{\delta E}{\delta x} = \frac{q}{\varepsilon}[(N_D - N_A) + (p - n)] \quad (2)$$

Where E = electric field, q = electronic charge, N_D= ionized donor density, N_A = ionized acceptor density, p = hole density, n = electron density, ε = permittivity of the semiconductor.

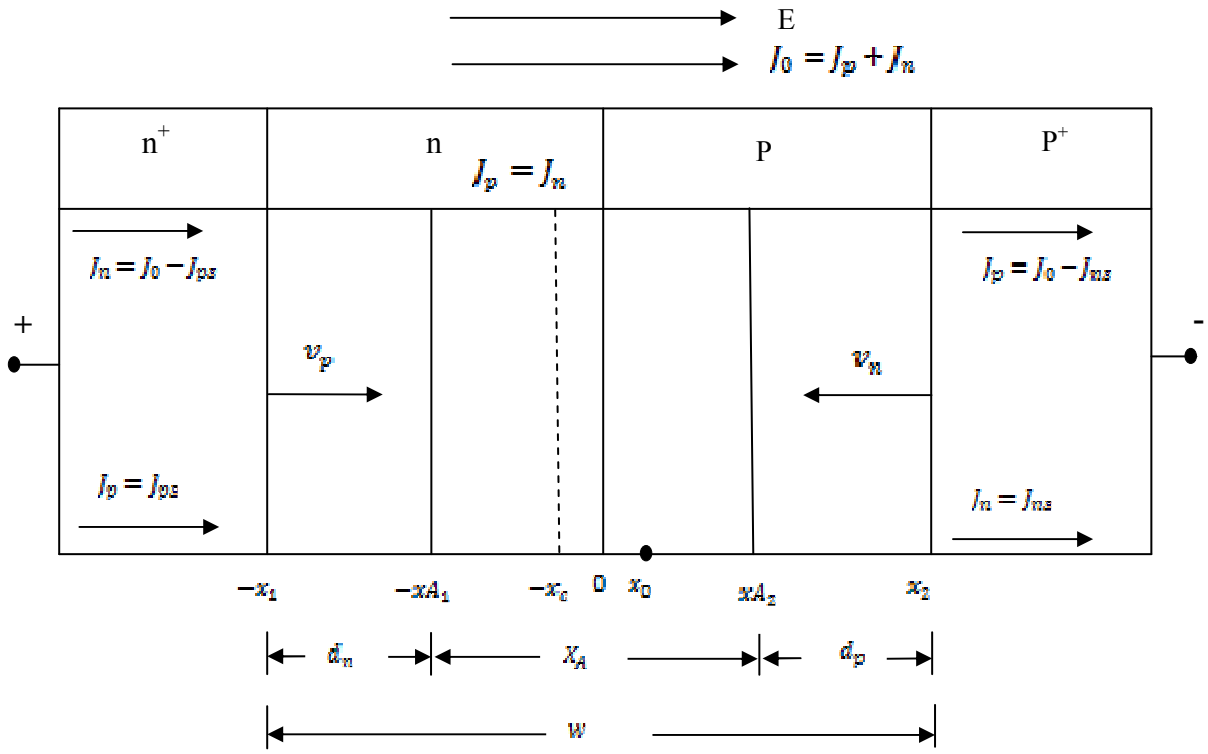

x_0 = Position of field maximum (E_0), x_c = Position of Avalanche centre$(J_p = J_n)$, w = Total active layer widths = $x_2 + |x_1|$, d_n, d_p= Drift layer widths for electrons and holes, x_A = Avalanche layer width = $x_{A2} + |x_{A1}|$, J_0 = Total current density = $(J_p + J_n)$

Figure 1 The active layer of a reverse biased p – n junction

The equations of continuity for electrons and holes are given by

$$\frac{\delta n}{\delta t} = \frac{1}{q}\frac{\delta J_n}{\delta x} + g \quad (3.a)$$

$$\frac{\delta p}{\delta t} = -\frac{1}{q}\frac{\delta J_n}{\delta x} + g \quad (3.b)$$

where g is the generation rate, $(\alpha_{n,p})$ is the ionization rate and $(v_{n,p})$ is the velocity of charge carriers.

The above mentioned parameters are expressed in the following equations

$$g = \alpha_n \cdot v_{sn} \cdot n + \alpha_p \cdot v_{sp} \cdot p \quad (3.c)$$

$$\alpha_{n,p} = A_{n,p} \cdot exp\left(-\frac{B_{n,p}}{E(x)}\right) \quad (3.d)$$

$$v_{n,p} = v_{sn,sp} \cdot \left[1 - exp\left(-\frac{\mu_{n,p} E(x)}{v_{sn,sp}}\right)\right] \quad (3.e)$$

where $v_{sn,sp}$ indicates the saturated drift velocity and $\mu_{n,p}$ is the mobility of charge carriers.

From the above equations the fundamental time and space dependent differential equation involving the electric field and the total current density under dynamic condition is given by

$$\left[\frac{\delta^2}{\delta x^2} - k^2 + \left\{(\alpha_n - \alpha_p) + \frac{\delta}{\delta E}(\alpha_n - \alpha_p).\vec{e} + 2.\bar{r}.k\right\}\frac{\delta}{\delta x} + 2.\bar{r}\,k\right].(E_m + \hat{e}) =$$

$$\frac{J_{dc} + \hat{J}_t}{\bar{v}.\varepsilon}\left[2.\left(\bar{\alpha} + \frac{\delta\alpha}{\delta E}\hat{e}\right) - k\right] \quad (4)$$

where

$$\bar{v} = (v_{sn} + v_{sp})^{1/2}$$

$$\bar{\alpha} = \frac{\alpha_n v_{sn} + \alpha_p v_{sp}}{2.\bar{v}}$$

$$\bar{r} = \frac{(v_{sn} + v_{sp})}{2.\bar{v}} \quad ,$$

$$k = j\omega,$$

$$H = \frac{J_{dc}}{\bar{v}.\varepsilon}\left[2.\frac{\delta\bar{\alpha}}{dE} + \frac{\bar{v}.\varepsilon}{J_{dc}} \cdot \frac{\delta E_m}{\delta x}\frac{\delta}{\delta E}(\alpha_n - \alpha_p)\right]$$

To linearize the non-linear Eq. (4), we introduce a parameter H [11] mentioned above. Hence

$$\left[\frac{\delta^2}{\delta x^2} + \frac{\omega^2}{\bar{v}^2} + \left\{(\alpha_n - \alpha_p) + j.2.\bar{r}.\frac{\omega}{v}\right\}\frac{\delta}{\delta x} + j.2.\bar{\alpha}\,\frac{\omega}{v} - H\right] Z(x,\omega) = \frac{1}{\bar{v}.\varepsilon}\left(2.\bar{\alpha} - \frac{j\omega}{v}\right) \quad (5)$$

where $Z(x,\omega) = \frac{\bar{e}}{j_t}$ = ac impedance.

Let the boundaries of p and n regions be at the co-ordinates $x = x_2$ and $x = -x_1$, respectively. Thus from Eq. (1), the boundary condition at $x = x_2$ (p region).

$$I_{total} = q.(\vec{p}.v_{sp}) + \frac{\delta}{\delta t}(\varepsilon.\vec{e}) \quad (6.a)$$

$$q.\vec{p} = \frac{\delta \varepsilon.\dot{e}}{\delta x} \quad (6.b)$$

from these two equations

$$\frac{1}{v_{sn}.\varepsilon} = \left(\frac{j\omega}{v_{sp}} + \frac{\delta}{\delta x}\right) Z(x,\omega) \quad (6.c)$$

at the left edge at $x = -x_1$(n region)

$$-\frac{1}{v_{sn}.\varepsilon} = \left(-\frac{j\omega}{v_{sn}} + \frac{\delta}{\delta x}\right) Z(x,\omega) \quad (6.d)$$

Considering $Z(x,\omega) = R + j.X$, and separating the real and imaginary parts, the following second order differential equations are obtained.

$$\frac{\delta^2 R}{\delta x^2} + \{\alpha_n(x) - \alpha_p(x)\}\frac{\delta R}{\delta x} - 2.\bar{r}\frac{\omega}{v}\frac{\delta R}{\delta x} + \left\{\frac{\omega^2}{v^2} - H(x)\right\}X + 2.\bar{\alpha}(x).\frac{\omega}{v}.R + \frac{\omega}{v^2.\varepsilon} = 0 \quad (7)$$

$$\frac{\delta^2 X}{\delta x^2} + \{\alpha_n(x) - \alpha_p(x)\}\frac{\delta X}{\delta x} + 2.\bar{r}.\frac{\omega}{v}.\frac{\delta R}{\delta x} + \left\{\frac{\omega^2}{v^2} - H(x)\right\} + 2.\bar{\alpha}(x).\frac{\omega}{v}.R + \frac{\omega}{v^2.\varepsilon} = 0 \quad (8)$$

The boundary conditions are, at $x = x_2$

$$\frac{\delta R}{\delta x} - \frac{\omega.X}{v_{sp}} = \frac{1}{v_{sp}.\varepsilon} \quad (9.a)$$

$$\frac{\delta X}{\delta x} + \frac{\omega.R}{v_{sp}} = 0 \quad (9.b)$$

Similarly at $x = -x_1$

$$\frac{\delta R}{\delta x} + \frac{\omega X}{v_{SYL}} = -\frac{1}{v_{SYL}.\varepsilon}$$

(9.c)

$$\frac{\delta X}{\delta x} - \frac{\omega R}{v_{SYL}} = 0$$

(9.d)

The device negative resistance and reactance are obtained from the following

$$Z_R = \int_0^W R.dx$$

(10.a)

and $Z_X = \int_0^W X.dx$

(10.b)

Conductance G = $\frac{Z_R}{Z_R^2 + Z_X^2}$

(11)

Susceptance B = $-\frac{Z_X}{Z_R^2 + Z_X^2}$

(12)

Quality factor $Q = -\left|\frac{B}{G}\right|$

(13)

The d.c. to r.f. conversion efficiency (η_d) of device has been calculated by [4-5]

$$\eta_d = \frac{1}{\pi} . \frac{V_B - V_A}{V_B}$$

(14)

where V_B and V_A indicate the values of breakdown and avalanche voltage of the diode respectively. This holds good satisfactorily upto a field variation of 50% of the maximum d.c. field value [4].

The estimated power from the diode can be calculated as

$$P_{est} = V_B . J_{dc} . A . \eta_d$$

(15)

where J_{dc} and A are the d.c. bias current density and diode area respectively.

2.1 Simulation Results

A standard Ka-band SDR (p^+nn^+) type silicon IMPATT diode has been designed considering the electron depletion layer width approximately by the equation $W_n = 0.37 \times V_{ns}/f$

where V_{ns} and f are the saturated electron velocity and f is frequency in GHz respectively. Realistic exponential and error function doping profiles at the device junction and at substrate-epitaxy contact region have been incorporated in the simulation . Standard experimental values of ionization rates [12], field dependent drift velocities and mobilities [13] of the charge carriers have been utilized for DC and Small signal simulation. The device parameters taken for the Ka-band simulation are shown in the Table:1. At a given bias current density, the peak frequency is the frequency at which the negative conductance of the diode is maximum. Thus the characteristics for the Small signal admittance of the diode, i.e., G-B plots; can be obtained for different frequencies at various values of d.c. bias current. The values of conductance (G_p), susceptance (B_p) , corresponding peak frequency (f_p) and device quality factor (Q) obtained from simulation in the small signal case as well as field swing upto 50% for Ka-band SDR IMPATT diode have been shown in Table:2. The Small signal admittance (G – B) plots obtained from the simulation have also been shown in Figure 2 and the field swing vs device quality factor (Q) in Figure 3.

Table: 1
Device parameter for Ka-band Simulation

W_n [μm]	N_d [m^{-3}]	Temp. [^oC]	Current density(J) [A/m^2]	Diode area(A) [m^2]
1.4	$2.5x10^{22}$	200	$6.0x10^7$	$0.226x10^{-8}$

Table: 2
Small signal simulation parameters at various field swings

Field swing (on E_m)	Peak freq. (f_p) [GHz]	Conductance (G_p) [mho/m^2]	Susceptance (B_p) [mho/m^2]	Quality factor (Q)
Small Signal case	36.2	$-25.88x10^5$	$106.90x10^5$	4.130
10%	36.2	$-23.81\ x10^5$	$107.14\ x10^5$	4.499
20%	36.0	$-21.66\ x10^5$	$107.62\ x10^5$	4.968
30%	36.0	$-20.14\ x10^5$	$107.84\ x10^5$	5.345
40%	36.0	$-19.14\ x10^5$	$108.12\ x10^5$	5.648
50%	36.0	$-18.37\ x10^5$	$108.30\ x10^5$	5.895

\

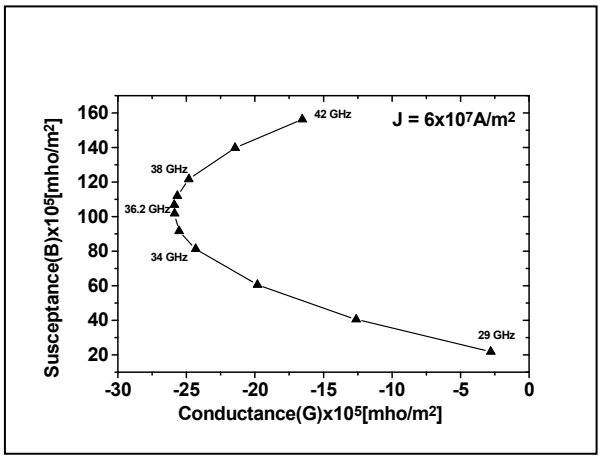

Figure 2. Admittance (G – B) plot from small signal simulation for Ka-band operation

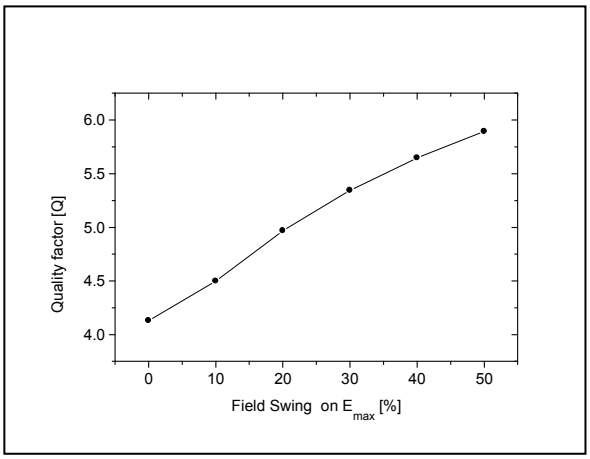

Figure 3. Plot of Field swing Vs Device Quality factor

3. Ka-band IMPATT Oscillator

For realizing an oscillator the IMPATT diode has been embedded in a microwave cavity and connected to the load through a matching network, schematically shown in Figure 4. (a). Figure 4.(b) shows the equivalent circuit of the IMPATT oscillator. It may be seen that the active device (i.e. the IMPATT diode) is represented by a negative conductance $-G_D$ in parallel with a capacitive susceptance B_D and the passive microwave circuit (i.e. the cavity and useful load), as viewed from the diode terminals, is represented by a positive conductance G_c in parallel with an inductive susceptance B_c. The oscillator consists of a device having admittance $Y_D = -G_D + jB_D$ and a circuit with admittance is $Y_c = G_c + jB_c$. Steady state condition of the oscillator can be written [5, 14].

$$G_D(V, \omega) - G_c(\omega) = 0 \quad (16)$$

$$B_D(V, \omega) + B_c(\omega) = 0 \quad (17)$$

The stability of the oscillator is ensured by the net zero conductance of the circuit-diode combination and the frequency of oscillation is determined by the resonant frequency of the system, where the total susceptance is zero.

The authors have used a resonant cap oscillator comprising a circular metallic cap placed in parallel with the broad face of the rectangular waveguide as shown schematically in Figure 5, details are described elsewhere [6] . The cap is set through a metal post into the waveguide cavity and the IMPATT diode is placed under the cap. The integrated heat sink of the diode is partially inserted into the rectangular waveguide to facilitate optimization. The waveguide is fitted with a variable sliding short at one end while the other end is connected to the passive load. The d.c. bias current feed to the device through a π-section low pass filter. The whole system is mechanically tunable through sliding back short tuner. Electronic tuning of the oscillator can be realized by varying the input d.c. bias current in steps from a constant current source. The generated r.f. signal from the IMPATT diode spreads radially outward and coupled to the rectangular waveguide through the open edge of the radial cavity formed

between the cap and the upper plane of the integrated heat sink. The photograph of the actual oscillator used in the study has been shown in Figure 6.

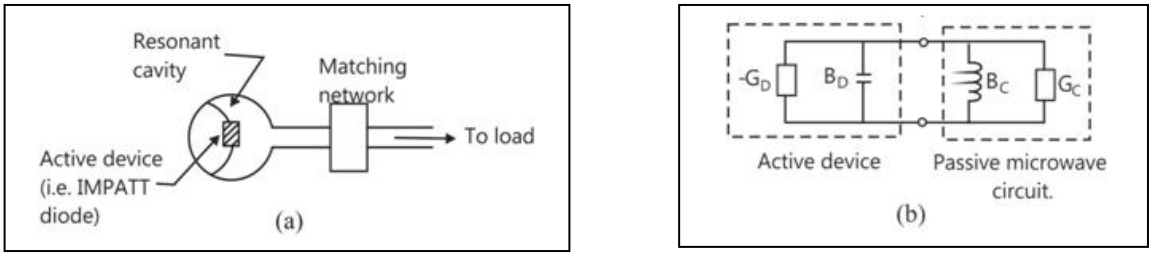

Figure 4. (a) Schematic diagram of IMPATT oscillator and (b) Equivalent circuit of the oscillator.

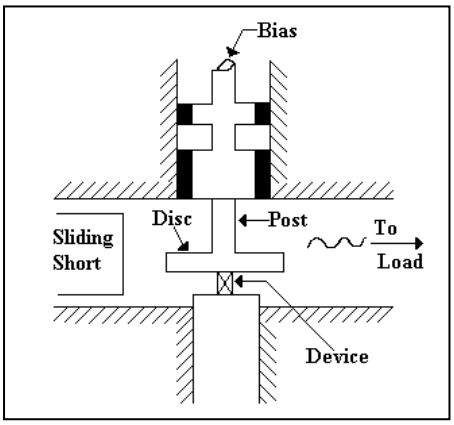

Figure 5. Schematic diagram of a Ka-band resonant cap cavity used [6]

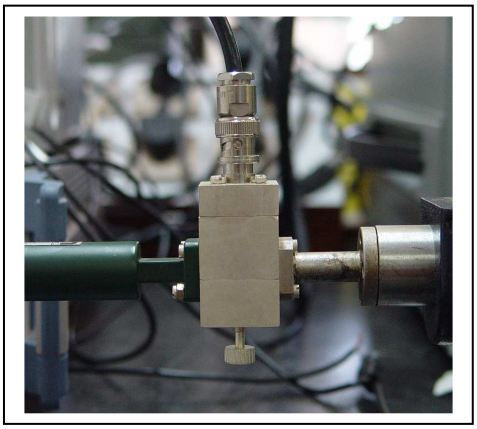

Figure 6. Photograph of the Ka-band resonant cap IMPATT oscillator

3.1 Experimental Studies and Results

The d.c. bias for the IMPATT diode is obtained from a constant-current power supply which can feed 0-500 mA current at 20-50 V break down voltage. The output power and frequency can be controlled by adjustment of cap height and cap diameter (cavity tuning) and by varying the d.c. current (electronic tuning) and by varying the position of a sliding short tuner (mechanical tuning). The authors have carried out experiment by varying the cap diameter in the range of 3.5 mm to 4.5 mm and the cap height in the range of 1.0 mm to 1.8 mm and also simultaneously varying the d.c. bias current and back short tuner position. Figure 7 shows the test set up used by the authors for optimization and characterization of the oscillator. The authors have achieved the optimized power output of 180 mW at 36.25 GHz as shown in Figure 8 with the combination of cap diameter = 4.0 mm and cap height =1.5 mm at d.c. bias current 180 mA and the back short tuner position 2.0 mm. A typical spectrum of indigenously developed Ka-band IMPATT oscillator is shown in Figure 9.

Thus the circuit efficiency (η_{ckt}) w.r.t optimum oscillator output power can be written as

$$\eta_{ckt} = \frac{P_{opt}}{P_{est}} \quad (18)$$

where P_{opt} = optimum oscillator output power
and P_{est} = estimated power of the device from simulation.

The estimated power from the device (P_{est}) and its efficiency (η_d) and circuit efficiency (η_{ckt}) w.r.t. optimum value of oscillator output for various field swings have been shown in Table: 3.

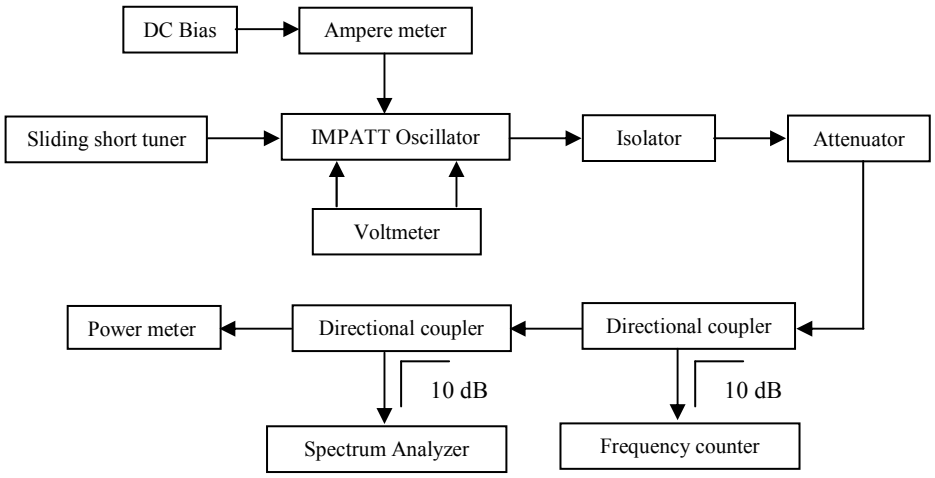

FIGURE 7. Block diagram of Ka-band Test set up

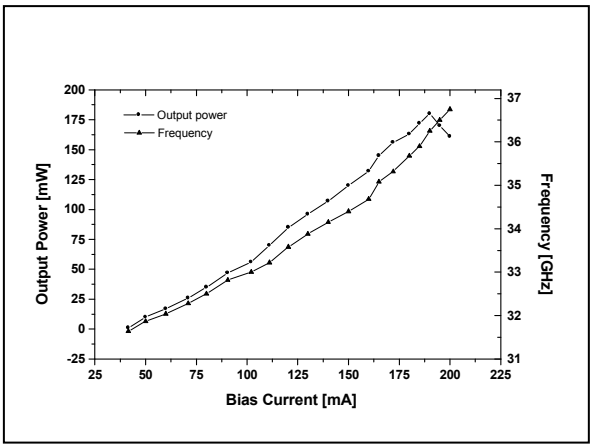

Figure 8. Experimental results: d.c. bias current Vs Frequency & Output power

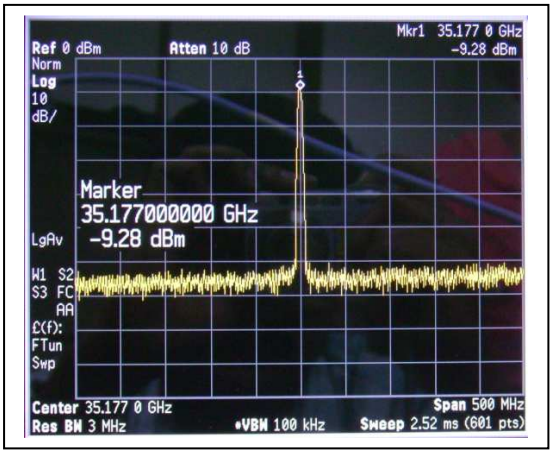

Figure 9. A typical spectrum of Ka-band IMPATT Oscillator

Table: 3
Device and Circuit efficiencies of Ka-band SDR (p^+nn^+) IMPATT diode at various field swings

Field swing (on E_m)	V_B [Volt]	V_A [Volt]	Device efficiency (η_d) [%]	P_{est} [mW]	Circuit efficiency η_{ckt} [%]
Small signal	36.5	26.20	8.98	444	40.54
10%	36.55	26.42	8.82	437	41.18
20%	36.60	26.63	8.67	430	41.86
30%	36.60	27.05	8.37	416	43.26
40%	36.75	27.43	8.08	402	44.77
50%	36.80	27.74	7.84	391	46.03

4. Conclusion

It has been concluded that the d.c. to r.f. conversion efficiency of the SDR IMPATT diode decreases with the increase in field swing. The value of the efficiency is found to be 8.98% for Small signal operation whereas its value becomes 7.84% for a field swing of 50% over the maximum d.c. field value. It has also been observed that the maximum value of negative conductance of the device progressively decreases with the increase in the field swing, while the device susceptance increases very slowly with the same and the device quality factor also increases linearly. The maximum output power obtained experimentally from the oscillator has been found to be 180 mW at the optimized condition. Its magnitude has been observed to fall rapidly with further increase in input d.c. bias current. An estimation of the r.f. power from the IMPATT diode has been made and a calculation of circuit efficiency w.r.t optimum value of oscillator output power for various field swings has been done. It is observed from the Table: 3 that the circuit efficiency varies between 40.54% and 46.03% for a moderate range of field swing upto 50% of the maximum d.c. electric field value, while the device efficiency falls with the increase in field swing. The results obtained around the optimum condition give an idea about the mutual relation between the device and circuit efficiencies and their interdependence.

It may thus be concluded that the low d.c. to r.f. conversion efficiency of the active device is mainly responsible for the low efficiency of the whole system whereas the present resonant cap system may be considered to be less responsible for it. Although the performance of the oscillator system can be improved with the better design of the active device as well as the mounting system, more emphasis should be given towards improving the conversion efficiency of the active IMPATT diode to achieve larger amount of oscillator output at optimized condition.

5. Acknowledgement

The author [1] is thankful to Shri. S.K. Ray, DS & Director, Research Centre Imarat, Hyderabad, Shri. R. Das, Director, RF Systems, Dr. V.G. Borkar, Head, Antenna & Components Group and Shri. J.V. Prasad, Head, MMW Seekers & Sensors Division for their consistent support and encouragement for carrying out the research work.

6. References

[1] S.K. Roy, "Transit Time Device", *"Encyclopaedia of Electron Devices"* vol. 24, Edited by John G. Webster, Wiley & Sons, New York, 1999.
[2] J.P. Banerjee, J.F. Luy and F. Schaffler, "Comparison of theoretical and experimental 60GHz silicon Impatt diode performance, Electronic Lett. (UK) Vol. 27, No. 12, pp. 1049-1051, 1991.
[3] Peter Russer, "Si and SiGe Millimeter-wave Integrated Circuits", *IEEE Trans. on MTT,* Vol. 46, No. 5, pp. 590-603, 1998.
[4] D.L. Sharfetter and H.K. Gummel, "Large signal analysis of a silicon Read diode oscillator", IEEE Trans. Electron Devices, Vol. ED- 16, No.1, pp.64-77, Jan.1969.
[5] G.Gibbons, "Avalanche diode microwave oscillators", Oxford University Press, Oxford 1973, Ch.4, pp. 45-65.
[6] Tapas Kumar Pal, "A Tunable Millimeter wave (Ka-Band) IMPATT Source Using an Integrated Heat Sink cum Waveguide mount", Patent no. 221758, INDIA, 03.07.2008.
[7] T.Misawa and N.D.Kenyon, "An oscillator circuit with cap structure for millimeter-wave IMPATT diodes", IEEE Trans. Microwave Theory and Tech., Vol. MTT-18, p.969, 1970.
[8] N.D.Kenyon, "Equivalent circuit and tuning characteristics of resonant-cap type IMPATT diode oscillator", 1973 European Microwave Conference Proceedings, Vol. A.1.1.
[9] G.A.Swartz, Y.S.Chiang, C.P.Wen and A.Gonzales, "Performance of p-type epitaxial silicon millimeter-wave IMPATT diodes", IEEE Trans. Electron Devices, Vol. ED-21, p. 165, 1974.
[10] S.K.Roy, J.P. Banerjee and S.P. Pati, "A computer analysis of the distribution of high frequency negative resistance in the depletion layer of IMPATT diodes", Proceedings of the conference on Numerical Analysis of Semiconductor Devices (NASECODE IV) (Dublin, Republic of Ireland: Bolle Press), p. 494, 1985.
[11] H.K.Gummel and J.L.Blue, "A small signal theory of avalanche noise in IMPATT diodes", *IEEE Trans. Electron Devices,* Vol. ED-14, pp. 569-580, 1967.
[12] W.N.Grant , "Electron and hole ionization rates in epitaxial silicon at high electric field", Solid State Electron, Vol. 16, p. 1189, 1973.
[13] C.Canali, G.Ottaviani and A.A.Quaranta, "Drift velocity of electron and holes and associated anisotropic effects in silicon", J. Phys. Chem. Solids, Vol. 32, p. 1707, 1971.
[14] C. Chao and G. I. Haddad, "Non-linear behavior and bias modulation of an IMPATT diode oscillator", IEEE Trans. Microwave Theory and Tech., Vol. MTT-21, p. 619, 1973.

Authors

Shri Tapas Kumar Pal, born in October, 1976 at Kolkata, obtained his M.Sc degree in Physics with specialization in Microwaves from University of Calcutta in 1999. He has worked as a Senior Research Fellow and Senior Scientist at Centre of Advanced Study in Radiophysics & Electronics, University of Calcutta for a period of 2.5 years from Feb 2000 onwards. Later he worked as an Examiner of Patents & Designs at Patent Office, Kolkata till July 2005. Presently he is working as a Scientist 'D' at Research Centre Imarat, DRDO. He is currently engaged in development of MMW Seeker. His special interests are Design and Development of MMW IMPATT Diodes, Oscillators and Amplifiers and their computer simulations. He has also been pursuing Ph.D (Tech) Degree at Institute of

Radiophysics & Electronics, University of Calcutta, on “Millimeter wave IMPATT Diodes and Oscillators”. He is a Life Member of IETE and Member of IEEE.

Dr J. P. Banerjee obtained B.Sc. (Hons.) and M.Sc. in Physics and Ph.D. in Radio Physics and Electronics from the University of Calcutta. He is presently a full Professor in the Institute of Radio Physics and Electronics, C.U. He is the recipient of Indian National Science Academy Award and Griffith Memorial Prize in Science of the Calcutta University in 1986. He is the principal co-author of more than 125 research papers in international journals in the fields of Semiconductor Science and Technology, Microwave and Millimeter wave avalanche transit time devices and Avalanche Photo-detectors. He has authored a text book on solid state electronic devices published by Vikas Publishing Ltd, New Delhi, India. He is a fellow of IETE, Senior Member of IEEE, a life member of the Society of EMI and EMC and Semiconductor Society, India. He served as a referee for various National and International technical journals.